Research on a Prediction Mechanism for Architectural Pathologies in Cultural Relic Masonry Buildings Within the Chinese Cold Climate Region

Guoqiang Wang, Songfu Liu(✉), and Yihan Wang

School of Architecture, Harbin Institute of Technology, 66 West Dazhi Street, Nangang District, Harbin 150000, China

Abstract. Architectural pathologies resulting from complex factors such as climatic parameters have had negative impacts on the protection and preservation of cultural relic masonry buildings. The study of correlations between the building's degree of damage and its construction date can reveal and even predict the development of architectural pathologies, which can help to protect cultural relic masonry buildings more effectively and specially. The aim of this research is to investigate the relevance and correlations between these two factors in cultural relic masonry buildings, and introduce the rate of change in heat transfer coefficient of building walls as a quantitative index that characterizes the severity of building pathologies. Based on the statistical method LS-SVM (Least Square-Support Vector Machine) implemented through machine learning in the computer field, a quantitative relevance model between these two factors (LS-SVM MODEL) was established, allowing for the prediction of the rate of change in the thermal transfer coefficient of building walls. In addition, considering how Harbin is representative of cold climate cities, the study region is limited to Harbin City.

Keywords: Architectural pathology · Prediction mechanism · Cultural buildings · Cold climate regions · Thermal transfer coefficient

1 Introduction

In China, its cold regions are widely distributed. According to statistics, China's cold regions have an area of 4.17 million square kilometers which accounts for 43.5% of China's total land area. A large number of heritage buildings are distributed across China's wide-range cold region and therefore cold bad weather greatly threatens the protection of heritage buildings. Therefore, it is very important to study frost damage and develop a prediction mechanism for heritage buildings in such regions. Here, the main pathologies of heritage buildings are related to frost damage. In particular, freeze-thaw cycles have caused much damage to the internal structure of the walls. The winter in the northern part of China has the characteristics of fast freezing, a long freezing period and high freeze-thaw frequency. The snow falls for a period of up to 7 months from

September or October of every year to next April, resulting in a long period of snowfall and freezing; according to statistics, there are approx. 120 freeze- thaw cycles occurring in northeast China every year on average (Liu and Chen 2016). Based on this, it can be estimated that heritage buildings in the cold regions of China have experienced up to ten thousand freeze-thaw cycles during their 100-year-plus existence. Freeze-thaw cycles will increase the porosity and water absorption of red bricks (Huan et al. 2014) and the porosity inside the red bricks directly affects the thermal transfer coefficient of building exterior walls. The thermal transfer coefficient refers to the heat transferred when it passes through an area of one square meter within 1 s, with an air temperature difference of 1 (K, °C) on both sides of the envelope under stable thermal transfer conditions, and is measured as watt per square meter per Kelvin or W/(m^2 K) (Liu 2009).

The thermal transfer coefficient of the building envelope is one of the important indicators of the building wall's insulation performance and also serves as an important indicator of the health status of historical buildings in cold regions. Therefore, this paper studies the pathological principles of masonry heritage buildings in cold regions, from the viewpoint of changes in the thermal transfer coefficient of external building walls.

There are many factors, including wall moisture content, that result in changes to the thermal transfer coefficient of exterior building walls, and which fall into the category of artificial and uncontrollable factors, so we cannot quantify and accurately grasp such information. But time is an intuitive direct parameter that can allow us to measure and affect the building pathologies. Therefore, this paper considers pathology as a quantity that varies as a function of time and the relationship between time and other parameters. This relationship is identified with a computer method which is called "time series analysis" in the computer field (Heather 2007). This technology has become more mature at the present time (Durbin and Koopman 2011).

2 Data Acquisition

2.1 Object of Study

For this study, 20 masonry buildings in the Harbin area have been selected for measuring their thermal transfer coefficients on site. These buildings were all constructed in a 60-year period from the 1900s to the 1960s and differ in terms of construction date and their wall thickness, but are almost consistent in regards to construction material, structure, surrounding artificial environment and other conditions. The distribution of these buildings in Harbin is shown in Fig. 1. The building materials used for these buildings are early red clay bricks with clay serving as the main component, accounting for about 65%. As shown in Fig. 2, such bricks feature a low degree of sintering, poor compactness, loose structure and strong water absorption, and may suffer a change in porosity under the action of freeze-thaw cycles, thereby causing the change in thermal transfer coefficient of the walls (Liu and Chen 2017).

2.2 Field Measurements

Measurement Methods and Principles. In this paper, the thermal transfer coefficient of the historical building envelope is measured with the heat flow meter method, which

Fig. 1. Distribution of the selected 20 buildings on a map of Harbin. Source: authors.

Cement sand Plaster (15mm)

The old red brick wall(545mm)

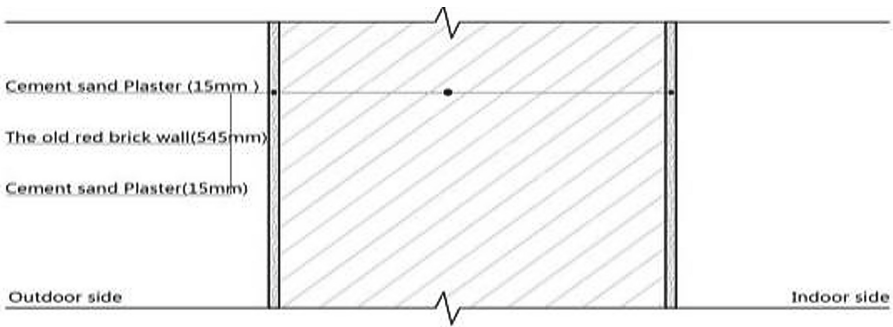Cement sand Plaster(15mm)

Outdoor side

Indoor side

Fig. 2. Diagram for standard structure of the walls of the selected buildings.

works as follows: The thermal transfer coefficient of the building envelope is measured based on the relationship between the thermal flux and thermal transfer temperature difference on both sides of the envelope. The thermal flux through the envelope is measured with a thermal flow meter sheet and the surface temperature on both sides of the envelope is measured with a temperature sensor. The thermal transfer coefficient of the envelope is calculated according to the thermal transfer principle. And the thermal transfer coefficient of the building envelope is measured to ensure that a certain thermal flux and thermal transfer temperature difference is formed on both sides of the envelope, and ensure that the indoor and outdoor temperature difference is higher than 20 °C so as to achieve a quasi-stable state of thermal transfer during winter heating (Shou 2015).

Measurement Position and Operation. In the process of testing, the selected test positions should not be located at thermal bridges, cracks, windows and other places vulnerable to the outdoor environment and should not be affected by heating or ventilation devices. The thermal flow meter should be installed in such a way that it is as close as possible to the surface of the envelope and the envelope surface should also be kept flat to the maximum possible extent. The meter is to be mounted by affixing it to the exterior

Table 1. On-site measurement results for the thermal transfer coefficients of building walls.

#	Building name	Structure type	Built year	Test year	Total years	Wall thickness	Heat transfer coefficient		Change value	Change rate
							Measured mean value	Theoretical mean value		
1	Clinic Building, Central Hospital of Harbin Railway Bureau	Brick-concrete	1900	2017	117	77	1.1865	0.9107	0.2758	30.279%
2	Distinguished Guesthouse of Longmen Mansion	Brick-wood	1904	2017	113	64.5	1.3984	1.0596	0.3388	31.979%
3	Electronic Entertainment Hall, Cultural Park	Brick-wood	1908	2017	109	77	1.1761	0.9107	0.2654	29.146%
4	Cultural Palace, Harbin Railway Bureau	Brick-concrete	1911	2017	106	77	1.1021	0.9107	0.1914	21.018%
5	Activity Center, Department of the Provincial Government	Brick-concrete	1914	2017	103	64.5	1.3808	1.0596	0.3212	30.312%
6	Glasses Store, Hengdeli	Brick-wood	1917	2017	100	54.5	1.1821	0.9107	0.2714	29.800%
7	No. 38 Residence, Hongjun Street	Brick-wood	1920	2017	97	54.5	1.5994	1.2191	0.3803	31.195%

(continued)

Table 1. (*continued*)

#	Building name	Structure type	Built year	Test year	Total years	Wall thickness	Heat transfer coefficient			
							Measured mean value	Theoretical mean value	Change value	Change rate
8	Foreign Economic & Trade Company, Harbin Railway Bureau	Brick-concrete	1925	2017	92	77	1.1523	0.9107	0.2416	26.523%
9	Federation Of Industry & Commerce, Harbin City	Brick-concrete	1927	2017	90	64.5	1.3263	1.0596	0.2667	25.167%
10	University of Humanities & Social Sciences, Harbin Institute of Technology	Brick-wood	1929	2017	88	64.5	1.3520	1.0596	0.2924	27.596%
11	Residence at No. 23, Xiajiash U Street	Brick-wood	1931	2017	86	54.5	1.5717	1.2191	0.3526	28.921%
12	Commercial and Residential Building, Jingyu Street	Brick-concrete	1933	2017	84	54.5	1.5610	1.2191	0.3419	28.044%

so as to ensure that the historical buildings are not damaged. The thermal flow meter should be affixed in such a way that the meter is closely attached onto the surfaces on both sides of the envelope, so that the clearance will not affect measurement accuracy (Liu et al. 2014). The temperature sensors are installed on the surfaces of both sides of the building envelope. The indoor temperature sensor should be located as close as possible to the thermal flow meter and the outdoor temperature sensor should be located at the position that corresponds with the position of the indoor heat flow sensor.

Furthermore, the thermal transfer coefficient was measured by selecting four vertical sides of a building in the process of measurement, and the measured values were averaged to obtain the mean value of the thermal transfer coefficient for the building's walls in order to ensure the universality of the test data. The impact of the building environment, orientation and special circumstances on the building heat transfer coefficient was minimized.

Measurement Results. Table 1 reports the on-site measurement results for the thermal transfer coefficients of building walls. The calculation results of the theoretical value of the wall thermal transfer coefficient are shown in Table 2.

Table 2. Calculation of the theoretical value of wall heat transfer coefficient.

Physical parameter	Signs	Unit	Formula	
Thermal transfer coefficients	K	W/(m^2 K)	K = 1/R0	
Thermal resistance	R0	(m^2 K)/W	R0 = Ri + $\sum$R + Re	
Internal surface thermal exchange resistance	Ri	(m^2 K)/W	Ri = 0.11	
Thermal exchange resistance of external surface	Re	(m^2 K)/W	Re = 0.04	
Thermal resistance of each material layer	$\sum$R	(m^2 K)/W	$\sum$R = R1 + R2 + R3	
	R1		R1 = d1/λ1	
	R2		R2 = d2/λ2	
	R3		R3 = d3/λ3	
Material thickness	d1	m	d1 = 15 mm	Cement sand plaster
	d2		d2 = 545 mm/645 mm/7 70 mm	Old red brick wall
	d3		d3 = 15 mm	Cement sand plaster
Thermal conductivity of materials	λ1		λ1 = 0.87	Cement sand plaster
	λ2		λ2 = 0.81	Old red brick wall
	λ3		λ3 = 0.87	Cement sand plaster

3   Method

A largely non-linear relationship exists between the building's completion date, wall thickness and rate of change in the wall's thermal transfer coefficient, that is, the rate of change in the thermal transfer coefficient does not simply increase with time, so an algorithm that fits a nonlinear variable relationship is required to predict the change tendency in the thermal transfer coefficient reasonably and accurately. To this effect, the LS-SVM (least-squares support-vector machine) method can identify the nonlinear relationship between building completion time, wall thickness and rate of change in the thermal transfer coefficient, and accurately predict the development of the rate of change in the thermal transfer coefficient, according to the time provided. Therefore, this paper predicted the change tendency of the thermal transfer coefficient of the wall based on the least-squares support-vector machine.

3.1   Fundamental Principle of LS-SVM

The LS-SVM algorithm sticks to the core principle of structural risk minimization of the support vector machine, and has solved such problems as the slow rate of convergence and long training time of the SVM algorithm. The solving of quadratic programming is converted into the solving of a linear equation set (Liu et al. 2014). For the given training sample set:

$$s = \{(x_1, y_1)(x_2, y_2), \ldots (x_n, y_n)\} \tag{1}$$

x_1 is the characteristic model input variable, y_1 is target variable, and n is sample size.

Generally, a non-linear relation exists between y and x. In order to realize the linear parameter regression, through a non-linear function ϕ (), the sample is mapped to a high-dimensional characteristic space, in which the set is:

$$\varphi(x) = (\phi(x_1), \phi(x_2) \ldots \phi(x_n)) \tag{2}$$

As for the selected RBF kernel function, the expression is,

$$K(x, y) = e\left(-\frac{(x-y)^2}{2\sigma^2}\right) \tag{3}$$

where σ is the kernel width parameter.

Subsequently, the linear regression is conducted for the training results in the high-dimensional characteristic space, the regression function being:

$$f(x) = w^T \cdot \phi(x) + b \tag{4}$$

where w^T is the weight vector, b is the offset value, and $\phi(x)$ is the non-linear function. After that, based on the structural risk minimization principle, the model parameters w and b are determined. The structural risk expression is:

$$R = \gamma \cdot R_{emp} + \frac{1}{2}\|w\|^2 R \tag{5}$$

where, γ is the regularization parameter, and $\gamma > 0$, R_{emp} is loss function or cost function; it is also called empirical risk function. The LS-SVM algorithm adopts the quadratic loss function:

$$R_{emp} = \sum_i^n \varepsilon_i^2 \tag{6}$$

where ε_i is the prediction error of the support vector machine model for the training sample.

The determination of model parameters w and b based on the structural risk minimization principle may be equivalent to the solving of the optimal parameter optimization under the structural risk minimization conditions:

$$y = w^T \cdot \phi(x) + b \tag{7}$$

The Lagrangian function (L) is introduced as,

$$L(w, b, \varepsilon_i, a) = \gamma \cdot \sum_i^n \varepsilon_i^2 + \frac{1}{2}\|w\|^2 - \sum_{i=1}^n \left(a_i \cdot \left(w^T \cdot \phi(x) + b - y_i\right)\right) \tag{8}$$

where a = [a1, a2,…an] is the Lagrangian multiplier. According to the optimization conditions:

$$\begin{cases} \frac{\partial L}{\partial w} = 0 \rightarrow w = \sum_{i=1}^n a_i \cdot \phi(x_i) \\ \frac{\partial L}{\partial b} = 0 \rightarrow \sum_{i=1}^n a_i = 0 \\ \frac{\partial L}{\partial \varepsilon_i} = 0 \rightarrow a_i = 2\gamma\varepsilon_i \\ \frac{\partial L}{\partial a_i} = 0 \rightarrow y_i = w^T \cdot \phi(x_i) + b + \varepsilon_i \end{cases} \tag{9}$$

After the systemization of Formula (9),

$$y_i = \sum_{j=1}^n \left(a_j \cdot \langle\phi(x_j), \phi(x_i)\rangle\right) + b + \frac{1}{2\gamma}a_i \tag{10}$$

After it is placed into a kernel function,

$$y_i = \sum_{j=1}^n \left(a_j \cdot K(x_i, x_j)\right) + b + \frac{1}{2\gamma}a_i \tag{11}$$

The simultaneous matrix form of linear equation set is as follows:

$$\begin{bmatrix} 0 & \mathbf{1}^T \\ \mathbf{1} \; K(x_i, x_j) + \gamma^{-1}I \end{bmatrix} \cdot \begin{bmatrix} b \\ a \end{bmatrix} = \begin{bmatrix} 0 \\ Y \end{bmatrix} \tag{12}$$

According to the training sample s = $\{(x_1, y_1) (x_2, y_2), \ldots (x_n, y_n)\}$, after formula (12) is solved, the values of a and b may be figured out. Finally, the function estimate of LS-SVM is:

$$f(x) = \sum_{j=1}^n a_j \cdot K(x_i, x_j) + b \tag{13}$$

Finally, after setting the features of the actual data set, we can obtain the input/output data model for the LS-SVM by means of kernel mapping, minimization of the risk factor and least square error criterion. By inputting the sample data, the model can be used to predict the rate of change in the thermal transfer coefficient of building walls.

3.2 Method Implementation

In Fig. 3, for the given change rate data of the thermal transfer coefficient, through this group of data, the characteristic variable and target variable should be built up first, and then the data are normalized. The normalization has the function of converting the original data into a standard normal distribution. The parameter setting involves the selection of the kernel and regularization parameters. The regularization parameter is used for balancing the loss function, and the kernel function is used for guaranteeing good linear characteristic mapping effects. The standardized data are mapped to a high-dimensional space through the kernel function.
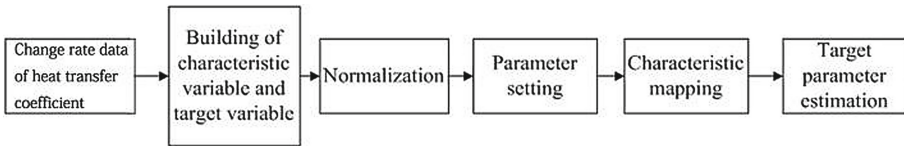
Fig. 3. Diagram of procedural steps for devising the thermal transfer coefficient prediction framework, based on a least-squares support-vector machine.

After the data are mapped to the high-dimensional space, the non-linear relation between the characteristic variable and target variable becomes a linear relation. Through the solution formula of LS-SVM, the mapping relation between them is made clear.

As for the characteristic mapping, through the selection of a linear function and a kernel function, the original data are linearly converted into the characteristic space, for the purpose of linear regression. As for the parameter estimation, by virtue of the characteristic sample, according to the function estimation formula (13), the parameter value is calculated.

Figure 4 illustrates the building pathology prediction process based on a least-squares support-vector machine. Firstly, the data is divided into the sample set and test set. The relationship between building completion time, wall thickness and rate of change is established by LS-SVM. The mathematical model is established according to the sample set, and the time and wall thickness of the test set are inputted into the model to obtain the prediction results for the rate of change. In order to verify the accuracy of the model, the error is obtained by comparing the predicted rate of change with the known rate of change in the test set. We can understand the rationality of the modelling and the accuracy of the prediction through error analysis.
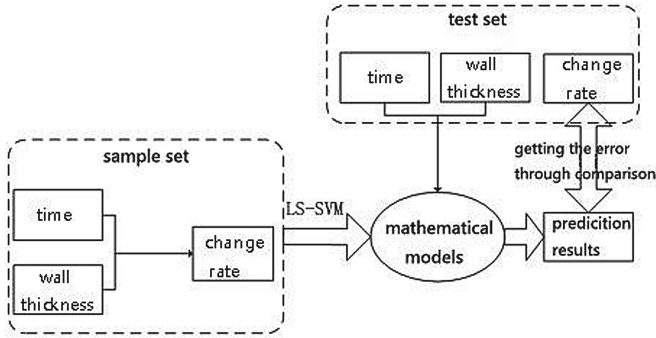
Fig. 4. Diagram explaining the thermal transfer coefficient prediction process, based on a least-squares support-vector machine

After the sample set and test set are selected, the characteristic and target variables are built, and the parameter values in the algorithm are reasonably set, the excellent performance of the algorithm may be guaranteed. Table 3 lists the input and output parameters of LS-SVM in the prediction of the change rate. After setting all of the parameters, we can train the sample data so as to build up the predictive model.

Table 3. Input and output parameters for the LS-SVM in the change rate prediction.

| Input parameters	Output parameters
Sample set of time, wall thickness, change rate	Change rate predicted value
Test set of time, wall thickness, change rate	
Regularization parameter: 69	
Kernel function parameter: 29 Kernel parameter: Gaussian radial basis kernel function	

4   Experiment Phase

In this paper, 20 buildings were measured on site in Harbin in order to verify the accuracy and rationality of the proposed method. The corresponding construction year, wall thickness and rate of change of these 20 buildings were respectively obtained. Due to the limited data that had been acquired, in order to fully verify the method proposed in this paper, the data for the 20 buildings was divided into 4 copies, with each copy containing the data of 5 buildings. Four experiments were conducted in total. For every experiment, one set of data is taken as a test set and the remaining three sets of data are taken as sample sets. In this way, the data for each building can be modelled as a sample set and can be verified as a test set.
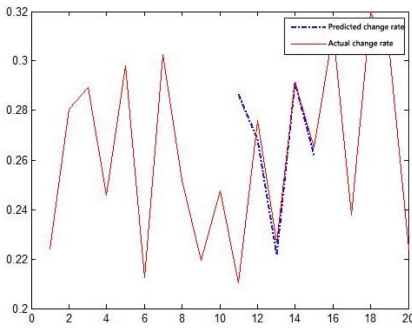
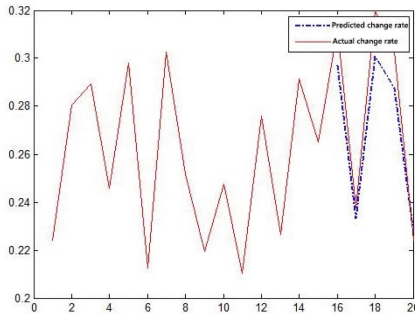The predicted results of the four experiments are shown in Fig. 5.
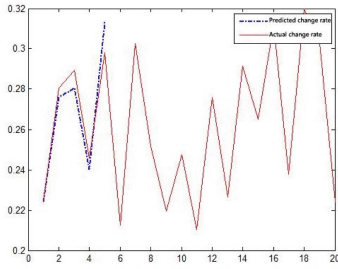
(a) Test and experiment results of the first group of buildings.
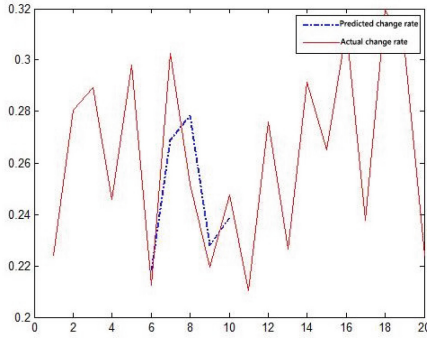
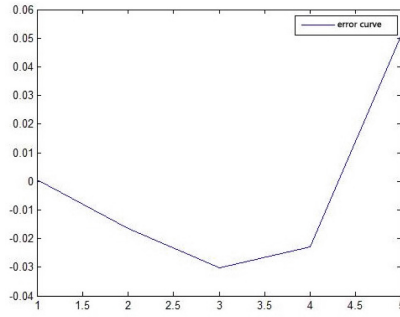(b) Test and experiment results of the second group of buildings.

(c) Test and experiment results of the third group of buildings.
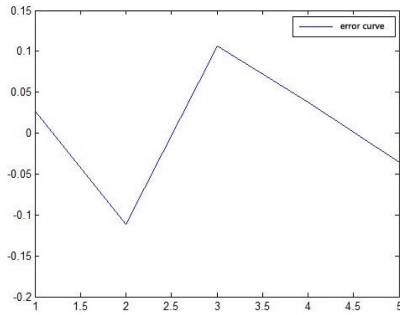

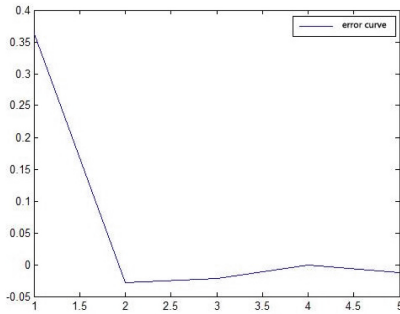(d) Test and experiment results of the fourth group of buildings.

Fig. 5. Results of the four tests and experiments for the 20 historic buildings.
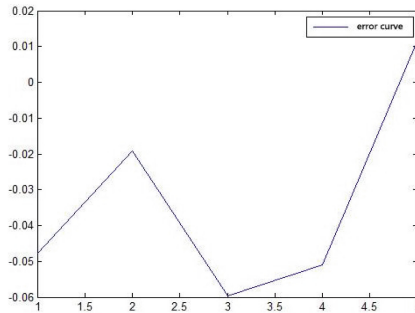
(a) Test and experiment error curve for the first group of buildings.

(b) Test and experiment error curve for the second group of buildings.

(c) Test and experiment error curve for the third group of buildings.

(d) Test and experiment error curve for the fourth group of buildings.

Fig. 6. Test and experiment error curves for the data set of 20 historic buildings.

The red solid line in the figure is the real rate of change curve for the 20 buildings, and the blue line is the rate of change predicted by the time and wall thickness relation provided by the corresponding buildings. It can be seen that the blue line can follow the red line very closely, indicating that the model established in this paper is accurate and thus we can predict the rate of change based on the time and wall thickness of the building. The corresponding prediction error curve is shown in Fig. 6.

From the four figures above, it can be seen that the error of the rate of change for each building is basically no more than 10%. The level of accuracy is high and relatively stable. This paper uses three error indicators to measure the accuracy of the algorithm: the mean square error, mean absolute error and mean error. The results are summarized in the Table 4:

Table 4. Statistics sheet for the three error indicators.

	1st Group	2nd Group	3rd Group	4th Group
MSE	0.0187	0.0417	0.1556	0.0209
MAE	0.0242	0.0637	0.0850	0.0379
ME	− 0.0035	0.0049	0.0600	− 0.0331

5   Conclusion

In this paper, the measured heat transfer coefficient values for the exterior walls of 20 masonry historical buildings (built in different years in the Harbin area) were obtained through an on-site measurement of the heat transfer coefficient of the exterior walls of these buildings, and the theoretical value of the heat transfer coefficient of the corresponding wall was calculated based on such parameters as the wall thickness of these buildings and the thermal conductivity of old red brick walls.

On the basis of these data, the mathematical model for the non-linear relationship between the building completion time, wall thickness and rate of change of thermal transfer coefficient was established with the least-squares support-vector machine (LS-SVM) algorithm. This allowed us to achieve the prediction of the tendency of change of the thermal transfer coefficient for the exterior walls of masonry heritage buildings in the cold regions of China. Furthermore, the actual data show that the predicted results obtained from the model have a high level of accuracy and stability. The application of the least-square support-vector machine method in the field of building pathology prediction provides effective technical and evidential support for the preventive protection of building heritage sites in the cold regions of China, which will further promote the development of the general protective measures for such cases.

References

Liu, S., Chen, S.: Mechanism of freezing-thawing on Chinese-Eastern railway heritage. J. South Archit. **2**, 26–32 (2016)

Huan, W., Zhang, Y., Liu, G., Zhao, P.: Performance deterioration and microstructure evolution of clay brick submitted to freeze thaw cycles. J. Southeast Univ. (Nat. Sci. Ed.) **44**(2), 401–405 (2014)

Liu, J.: Building Physics, 4th edn. China Architecture and Building Press, Beijing (2009)

Heather, M.A.: New introduction to multiple time series analysis by Helmut Lütkepoh (book review). Econ. Rec. **83**(260), 109–110 (2007). https://doi.org/10.1111/j.1475-4932.2007.003 84.x

Durbin, J., Koopman, S.J.: Time Series Analysis by State Space Methods, 2nd edn. Oup Catalogue, Oxford (2011). 39(461), 255–256

Ruping, S.: SVM kernels for time series analysis. Technical reports (2001). http://dx.doi.org/10. 17877/DE290R-15237

Liu, S., Chen, S.: The impact of meteorological parameters on salt efflorescence damage of historic architecture in cold regions. Archit. J. (2), 11–15 (2017)

Shou, X.: The on-site test of heat transfer coefficient of building envelope and analysis of heat transfer process. Master's thesis (2015)

Liu, L., Lin, X., Cai, Q., Jia, X., Yu, G.: Effects of testing position on identification accuracy of the wall heat transfer coefficient using the least square method. Build. Energy Effic. (3), 41–45 (2014)